

Influence of surface pretreatment on phosphate conversion coating on AZ91 Mg alloy

Zhang, Chunyan; Liu, Bin; Yu, Baoxing; Lu, Xiaopeng; Wei, Yong; Zhang, Tao; Mol, J. M.C.; Wang, Fuhui

DOI

[10.1016/j.surfcoat.2018.12.091](https://doi.org/10.1016/j.surfcoat.2018.12.091)

Publication date

2019

Document Version

Final published version

Published in

Surface and Coatings Technology

Citation (APA)

Zhang, C., Liu, B., Yu, B., Lu, X., Wei, Y., Zhang, T., Mol, J. M. C., & Wang, F. (2019). Influence of surface pretreatment on phosphate conversion coating on AZ91 Mg alloy. *Surface and Coatings Technology*, 359, 414-425. <https://doi.org/10.1016/j.surfcoat.2018.12.091>

Important note

To cite this publication, please use the final published version (if applicable).
Please check the document version above.

Copyright

Other than for strictly personal use, it is not permitted to download, forward or distribute the text or part of it, without the consent of the author(s) and/or copyright holder(s), unless the work is under an open content license such as Creative Commons.

Takedown policy

Please contact us and provide details if you believe this document breaches copyrights.
We will remove access to the work immediately and investigate your claim.

Green Open Access added to TU Delft Institutional Repository

'You share, we take care!' - Taverne project

<https://www.openaccess.nl/en/you-share-we-take-care>

Otherwise as indicated in the copyright section: the publisher is the copyright holder of this work and the author uses the Dutch legislation to make this work public.



Influence of surface pretreatment on phosphate conversion coating on AZ91 Mg alloy

Chunyan Zhang^{a,b}, Bin Liu^a, Baoxing Yu^b, Xiaopeng Lu^{c,*}, Yong Wei^a, Tao Zhang^{a,b,c,**}, J.M.C. Mol^d, Fuhui Wang^c

^a Corrosion and protection Laboratory, Key Laboratory of Superlight Materials and Surface Technology (Ministry of Education), Harbin Engineering University, Nantong ST 145, Harbin 150001, China

^b Corrosion and Protection Division, Shenyang National Laboratory for Materials Science, Institute of Metal Research, Shenyang 110016, China

^c Corrosion and Protection Division, Shenyang National Laboratory for Materials Science, Northeastern University, 3-11 Wenhua Road, Shenyang 110819, China

^d Delft University of Technology, Department of Materials Science and Engineering, Mekelweg 2, 2628 CD Delft, the Netherlands

ARTICLE INFO

Keywords:

Mg alloy
Phosphate conversion coating
Surface pretreatment
Corrosion protection

ABSTRACT

Surface pretreatment is generally applied before application of protective coatings on Mg alloys, which influences surface microstructure and electrochemical activity of the substrate and has an effect on the coating properties. The effect of various pretreatment processes (sand-blasting, grinding and polishing) on the microstructure and corrosion protection performance of phosphate conversion coating (PCC) on AZ91D Mg alloy was investigated in the present study. Sand-blasting cleaning significantly increases the surface roughness and electrochemical activity of the substrate, leading to formation of a porous PCC with inferior corrosion protection performance. In the case of ground/polished Mg alloy, the uniformity and corrosion resistance of the resultant conversion coating are mainly related to the surface roughness. Relatively low surface roughness of the substrate facilitates formation of a corrosion protective PCC.

1. Introduction

Mg alloys are of great potential to be used in automotive industry, aerospace and biomedical applications due to high specific strength, excellent machinability and biocompatibility [1–5]. However, poor corrosion and wear resistance are the main obstacles restricting the long-term performance and utilization of Mg alloys. A surface treatment process is generally applied to provide corrosion and wear protection for Mg alloys [6–10]. Conversion coatings are of high interest due to their industrial maturity and ease of application [11–13], which are formed by combined anodic dissolution and deposition of phosphate crystals and/or amorphous metal oxides on the metal surface during immersion in the treatment solution [14,15]. Chromate conversion coating has shown excellent corrosion resistance and self-healing ability, however it is subject to strict international health and safety legislation due to the toxicity and carcinogenicity of hexavalent chromium based chemistries [16,17]. Therefore, non-hexavalent chromium based conversion coatings are becoming more readily available at a commercial level and research into environmentally acceptable

alternatives has led to development of phosphate, fluoride and rare earth conversion coatings [18–20]. Optimization of the composition and concentration of the conversion bath is proved to have a huge effect on the composition and corrosion resistance of conversion coatings [21–24].

Prior to immersion in the conversion solution, surface pre-conditioning by alkaline and/or acid cleaning, mechanical pretreatment is commonly applied to remove organic contaminants, which are also typically part of the industrial manufacturing processes [25–27]. The microstructure, composition and electrochemical activity of the metal surface are modified and changed accordingly. It was found that surface pre-conditioning treatment influences the electrochemical surface activity and formation process of Zr-based conversion coatings formed on Al alloy [28,29]. Unfortunately, such effects have not been systematically investigated for conversion coatings on Mg in detail so far. In the present study, sand-blasting, grinding and polishing are applied on AZ91 Mg alloy to study the effect of surface pretreatment on the microstructure, composition and corrosion performance of phosphate conversion coating (PCC). It is known that formation of PCC on

* Corresponding author.

** Correspondence to: T. Zhang, Corrosion and protection Laboratory, Key Laboratory of Superlight Materials and Surface Technology (Ministry of Education), Harbin Engineering University, Nantong ST 145, Harbin 150001, China.

E-mail addresses: luxiaopeng@mail.neu.edu.cn (X. Lu), zhangtao@mail.neu.edu.cn (T. Zhang).

<https://doi.org/10.1016/j.surfcoat.2018.12.091>

Received 30 September 2018; Received in revised form 18 December 2018; Accepted 21 December 2018

Available online 22 December 2018

0257-8972/ © 2018 Elsevier B.V. All rights reserved.

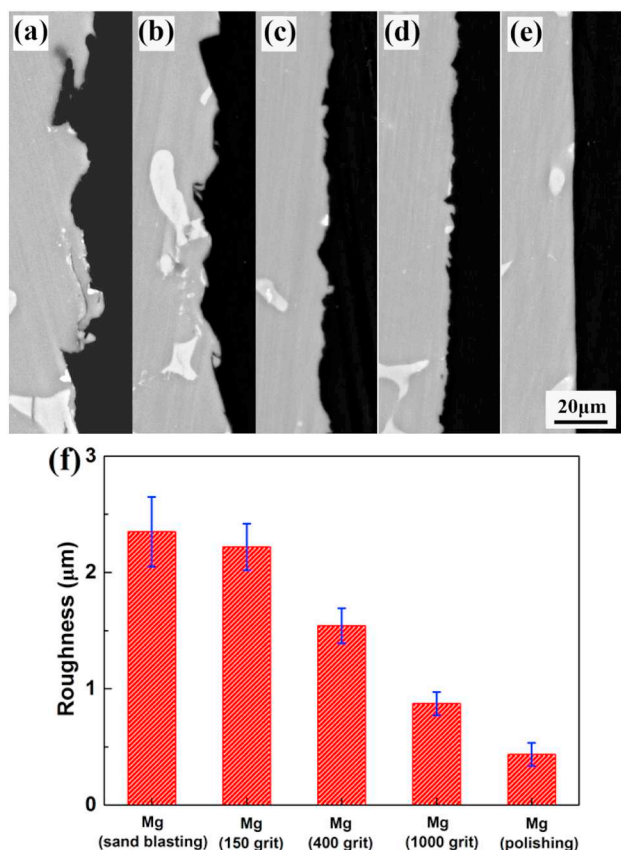


Fig. 1. Cross-sectional morphology and surface roughness of the pretreated Mg alloy. (a) Mg (sand-blasting), (b) Mg (150 grit), (c) Mg (400 grit), (d) Mg (1000 grit), (e) Mg (polishing) and (f) surface roughness of the pretreated Mg alloy.

Mg alloys is an electrochemical dissolution and chemical deposition process [30]. Dissolution of Mg occurs once the alloy is immersed in the conversion bath. The pretreatment process might affect the microstructure and electrochemical activity of the Mg alloy surface, and subsequently influence Mg dissolution and deposition of insoluble phosphate compounds.

2. Experimental

2.1. Material and surface pretreatment

AZ91D Mg cast ingot was used in the present study. The composition of the alloy is 9.23 wt% Al, 0.73 wt% Zn, 0.21 wt% Mn, 0.029 wt% Si, 0.0014 wt% Fe, 0.0018 wt% Cu and Mg balance (ICP Optima 8300, Singapore). Sand-blasting pretreatment was carried out using a handheld Navite 872 with air pressure of 0.2 MPa for 2 min and corundum particles (180 μm) were used as the charging material. Mg alloy was ground up to 150, 400 and 1000 grit by silicon carbide paper, and was polished (2.5 μm alumina slurry) to study the effect of surface

roughness on the conversion coatings. The specimens were rinsed with ethanol and dried before formation of PCC. The surface roughness (R_a) of the sample was measured by a roughometer (MarSurf PS10, Mahr, Germany).

2.2. Fabrication of conversion coatings

The conversion bath was composed of 35 g/L NaH_2PO_4 , 5 g/L $(\text{NH}_4)_2\text{HPO}_4$, 2 g/L NaNO_3 and 35 g/L MnSO_4 . The alloy was treated for 10 min at a constant temperature of 60 °C. The pH value of the conversion bath was maintained at 3.5. The corresponding uncoated and coated Mg samples are named as Mg/PCC (sand-blasting), Mg/PCC (150 grit), Mg/PCC (400 grit), Mg/PCC (1000 grit) and Mg/PCC (polishing), respectively.

2.3. Microstructure and composition characterization

The surface and cross section morphology of the coatings were investigated by field-emission scanning electron microscopy (SEM, PHILIPS XL-30FEG) equipped with an energy dispersive spectrometer (EDS). The phase composition of the coatings was identified using X-ray diffraction (XRD, PHILIPS, PW1700, $\text{Cu K}\alpha_1$ radiation, $\lambda = 1.5406 \text{ \AA}$, 30 mA, 40 kV). The elemental distribution and composition in the cross section of the layer were studied and analyzed by electron probe microanalysis (EPMA, SHIMADZU, 1610). The surface microstructure and composition of the alloy after pretreatment process were investigated by transmission electron microscopy (TEM, JEOL, JEM-2100F). The sample preparation procedure can be found in our previous work [30].

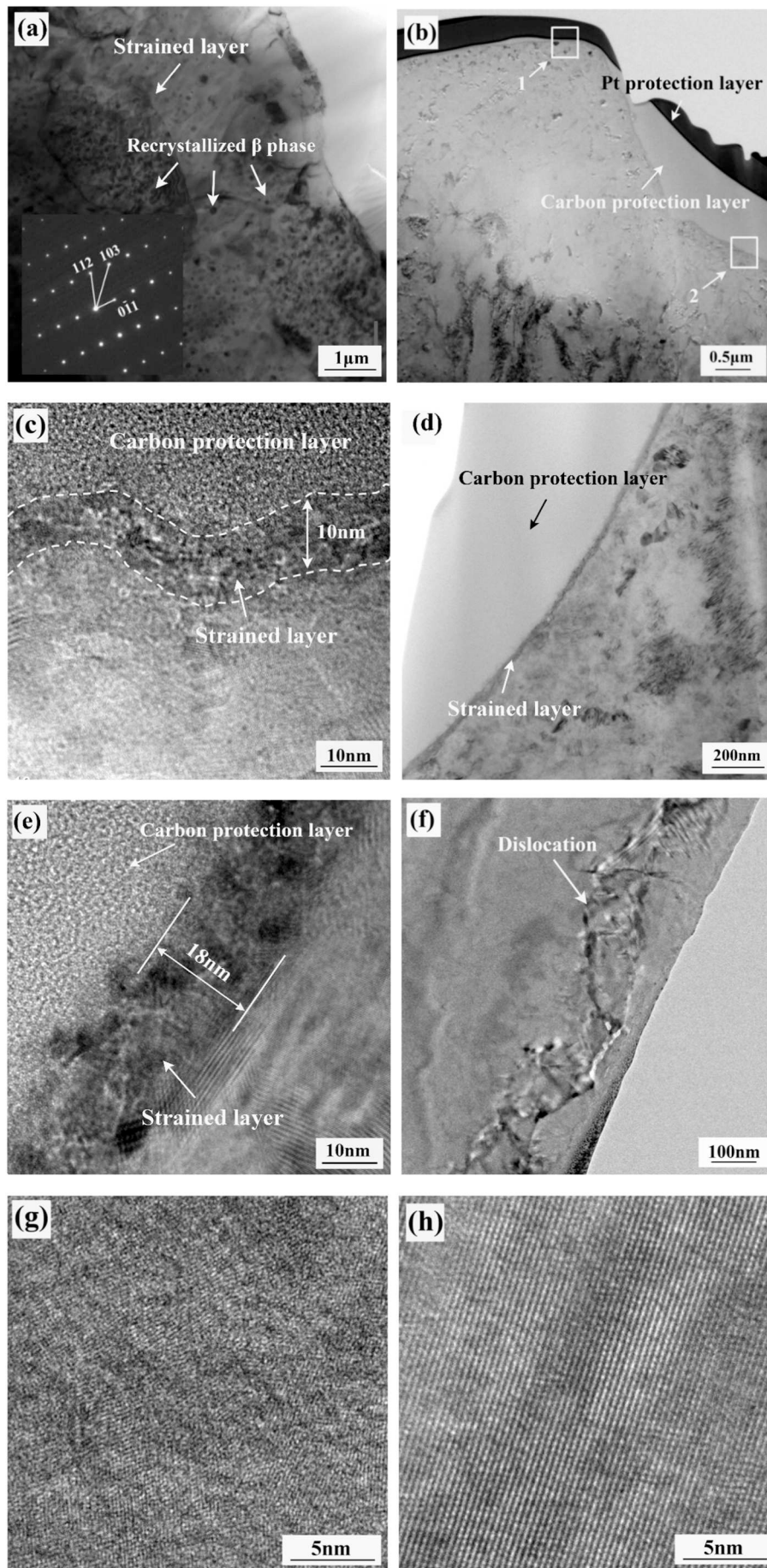
2.4. Evaluation of corrosion performance

The potentiodynamic polarization of the bare and coated Mg alloy was performed in an electrochemical workstation (Zennium), which consisted of a platinum foil as the counter electrode and a saturated calomel electrode (SCE, saturated KCl) as the reference electrode in 3.5 wt% NaCl solution. The coatings were polarized separately towards anodic and cathodic direction from the open circuit potential (after immersion around 20 min) with a scan rate of $0.333 \text{ mV}\cdot\text{s}^{-1}$. Hydrogen evolution analysis and salt spray testing were carried out to determine the corrosion protection performance of the conversion coatings. Hydrogen evolution test was performed by using eudiometers (Shu Niu Glass Instrument Co. Ltd) for 48 h at room temperature. The neutral salt spray test was performed for 48 h based on ASTM B117-03 standard. The macroscopic morphology of the uncoated and coated samples was obtained using a digital camera. Each measurement was repeated at least three times at room temperature to study the reproducibility of the measurements.

3. Results

3.1. Effect of pretreatment process on the surface microstructure and electrochemical activity of AZ91 Mg

The cross-sectional morphology and surface roughness (R_a) of the pretreated Mg alloy is shown in Fig. 1. It is apparent that the roughness



(caption on next page)

Fig. 2. TEM images of the surface microstructure of the pretreated alloy. (a) Mg (sand-blasting), (b, c, d and e) Mg (150 grit), (c) high resolution image of Region 1, (d and e) high resolution image of Region 2, (f, g and h) Mg (polishing), high resolution image of (g) dislocation on the Mg surface and (h) bulk material below the deformed surface layer.

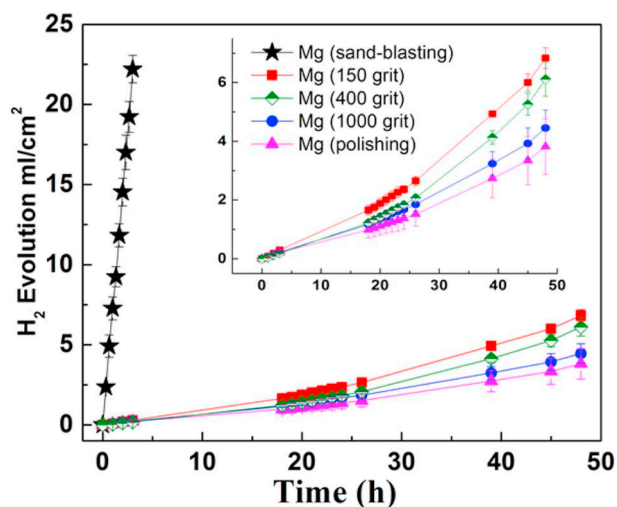


Fig. 3. Hydrogen evolution of the pretreated Mg alloy in 3.5 wt% NaCl solution.

of the substrate is higher after sand-blasting pretreatment and 150 grit grinding compared to the other samples. The roughness of Mg (1000 grit) and the polished alloy is the lowest among all the pretreated samples. It was reported that mechanical pretreatment can induce near surface plastic deformation and dislocations [31], which alters the microstructure and the electrochemical activity of the Mg alloy surface. Therefore, TEM was performed to investigate the microstructure of the pretreated samples (Fig. 2). A large number of newly recrystallized β phase has been detected on the sample treated by sand-blasting (Fig. 2a), which might lead to micro-galvanic corrosion and poor corrosion performance of the sample. It was found that the entire surface of the Mg alloy (sand-blasting) is covered by a strained and recrystallized layer (above $5\ \mu\text{m}$). As for the Mg alloy (150 grit), grinding induced a peak-to-valley structure (Fig. 2b), indicating a high surface roughness of the sample. A thin layer with lattice distortion and dislocations (Fig. 2c, d and e) can be observed at the surface of the ground alloy. The thickness of the strained layer at the valley (Fig. 2e) is slightly thicker compared to that on the peak (Fig. 2c). For the polished specimen, the Mg alloy surface is also modified and covered by dislocations and a strained layer (Fig. 2f and g), which is much thicker compared to that of the ground sample. The TEM analysis verifies that the applied pretreatment process changes the surface microstructure and roughness of the substrate. Specifically, the surface microstructure and composition of the sample is significantly modified by the sand-blasting pretreatment. The electrochemical activity of the pretreated samples is studied

by a hydrogen evolution analysis (Fig. 3). It can be observable that the corrosion rate of Mg alloy (sand-blasting) is significantly higher than that of the ground and polished alloy and the electrochemical activity of the alloy decreases with the surface roughness, which depends on the surface pretreatment process. The Mg dissolution rate increases significantly when there is a thick and deformed surface layer with a relatively high concentration of recrystallized β phases after the pretreatment process.

3.2. Effect of surface pretreatment on the microstructure and composition of PCC

Surface morphology of the conversion coatings is shown in Fig. 4. Some large-sized spherical particles are randomly detected on the surface of PCC (150 grit), which is proved to be Mn containing phosphate by EDS analysis (Mn: 17.3 at.%, P: 18.2 at.% and O: 64.5 at.%). The grain size of PCC (1000 grit) seems to be smaller and the coating is more uniform and denser compared to other coatings. The cross section of the coatings is presented in Fig. 5. It can be seen that the coating formed on the alloy with lower roughness is more homogeneous and denser (Fig. 5d and e) than that formed on the rougher Mg alloy surface (Fig. 5a, b and c). The cross-sectional morphology of PCC (150 grit) is consistent with the surface microstructure. The layer is non-uniform and the MnHPO_4 particles are mainly formed at the top region of the peak-to-valley structure. PCC (1000 grit) and PCC (polishing) are more uniform and compact, although the coating is thinner compared to PCC (400 grit). As for the coating composition, MgHPO_4 and MnHPO_4 have been detected to be the main phases for all the conversion coatings (Fig. 6), indicating that the phase composition of the conversion coating is not influenced by the surface pretreatment process. EPMA mappings were performed to further investigate the coating composition and element distribution (Fig. 7). It is apparent that the coating consists of an inner MgHPO_4 layer and an outer MnHPO_4 layer. In conclusion, the surface and cross-sectional microstructure of the conversion coatings is significantly influenced by the pretreatment process, although the phase composition and elemental distribution of the coating is marginally changed.

3.3. Corrosion resistance of the conversion coated Mg alloy

The polarization curves of the conversion coated Mg alloy and the corrosion current density (i_{corr}) determined from the cathodic branch by Tafel extrapolation are shown in Fig. 8 and Table 1, respectively. It can be seen that the corrosion current density of PCC (sand-blasting) is much higher compared to that of other conversion coatings. There is a slight difference among the conversion coatings formed on the ground and polished alloy. Hydrogen evolution analysis (Fig. 9) and salt spray testing (Fig. 10) were carried out to evaluate the long-term corrosion

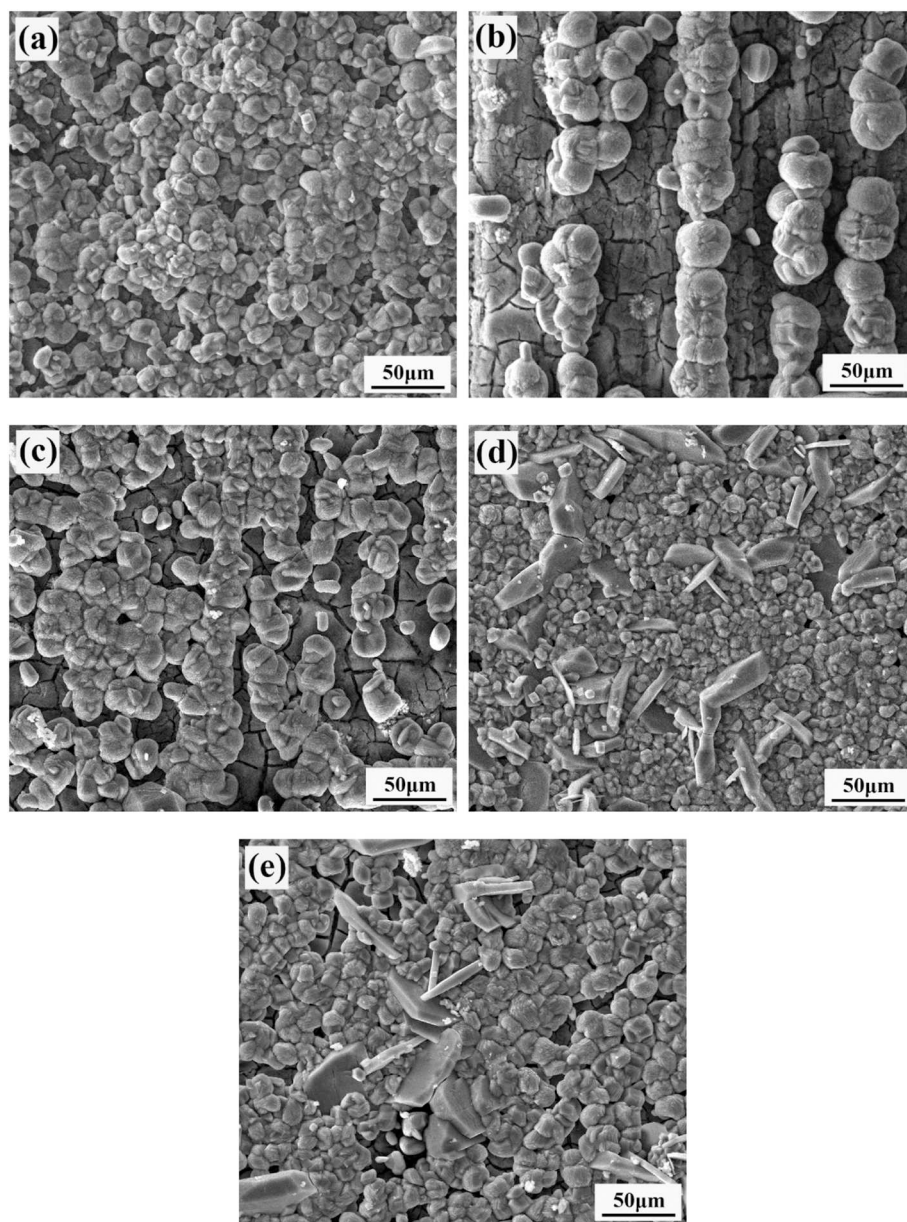


Fig. 4. Surface morphology of the conversion coatings. (a) PCC (sand-blasting), (b) PCC (150 grit), (c) PCC (400 grit), (d) PCC (1000 grit) and (e) PCC (polishing).

performance of the conversion coatings. It was found that the hydrogen evolution volume of PCC (1000 grit) and PCC (polishing) is lower than that of other coatings, which is consistent with the polarization measurement. The macroscopic morphology of the coatings before and after salt spray testing is shown in Fig. 10. It was evident that sand-blasting pretreatment is detrimental to the corrosion performance of phosphate

conversion coating. There are plenty of large-sized corrosion pits on the surface of PCC (150 grit) and PCC (400 grit) after 48 h corrosion testing. PCC (1000 grit) and PCC (polishing) start to be corroded after 72 h, indicating that the corrosion protection of the conversion coating increases with the decrease of the surface roughness of the treated Mg alloy.

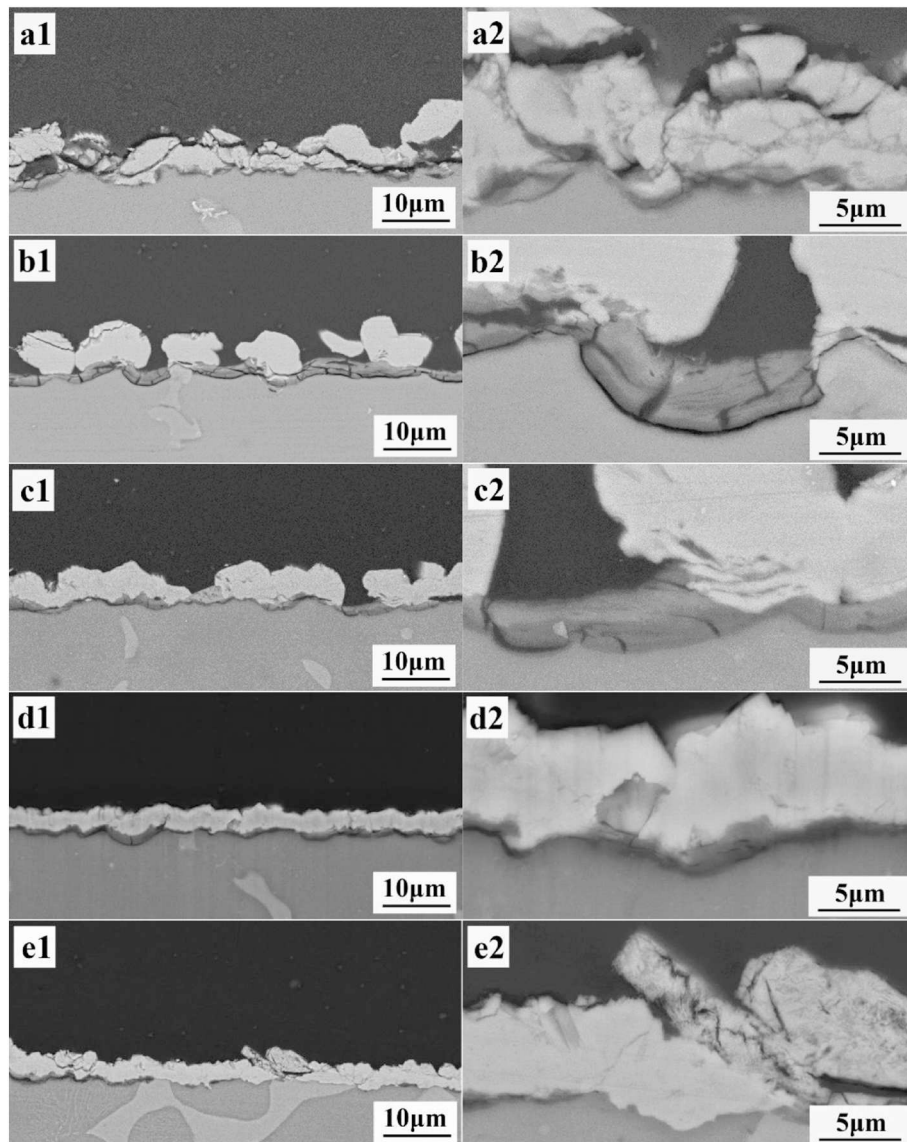


Fig. 5. Cross-sectional morphology of the conversion coatings. (a) PCC (sand-blasting), (b) PCC (150 grit), (c) PCC (400 grit), (d) PCC (1000 grit) and (e) PCC (polishing).

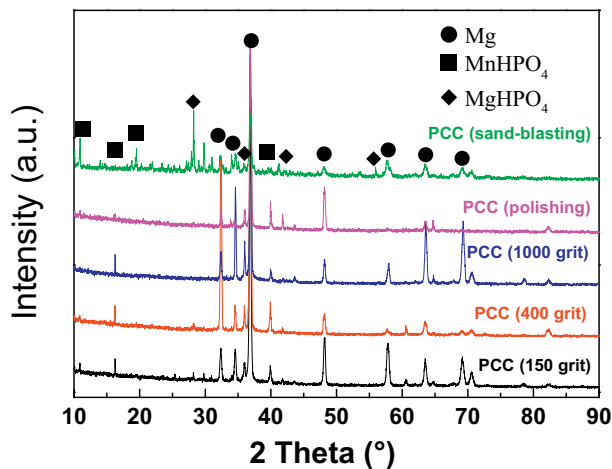


Fig. 6. XRD patterns of the conversion coatings.

4. Discussion

It is known that formation of phosphate conversion coatings on Mg is a combined electrochemical dissolution and chemical deposition process [32–34]. Dissolution of Mg occurs once the alloy is immersed in the conversion solution, while hydrogen evolution is accompanied as the main cathodic reaction, as listed in Table 2. Insoluble phosphate-based compounds via chemical reaction start to deposit on Mg surface afterwards. Therefore, the coating formation process and coating properties primarily depend on the surface microstructure and electrochemical activity of Mg alloy, which is related to the microstructure and composition of the substrate and can be altered by the pre-conditioning treatment. It can be deduced that the peak-to-valley structure of the ground sample is beneficial to deposition and nucleation of MgHPO_4 since the diffusion of the dissolved Mg ions is suppressed at the valley which is similar to the diffusion in a pitting cavity [35]. Similarly, the peak region facilitates formation of MnHPO_4 rather than MgHPO_4 , as shown in Fig. 11. In the case of the substrate with low

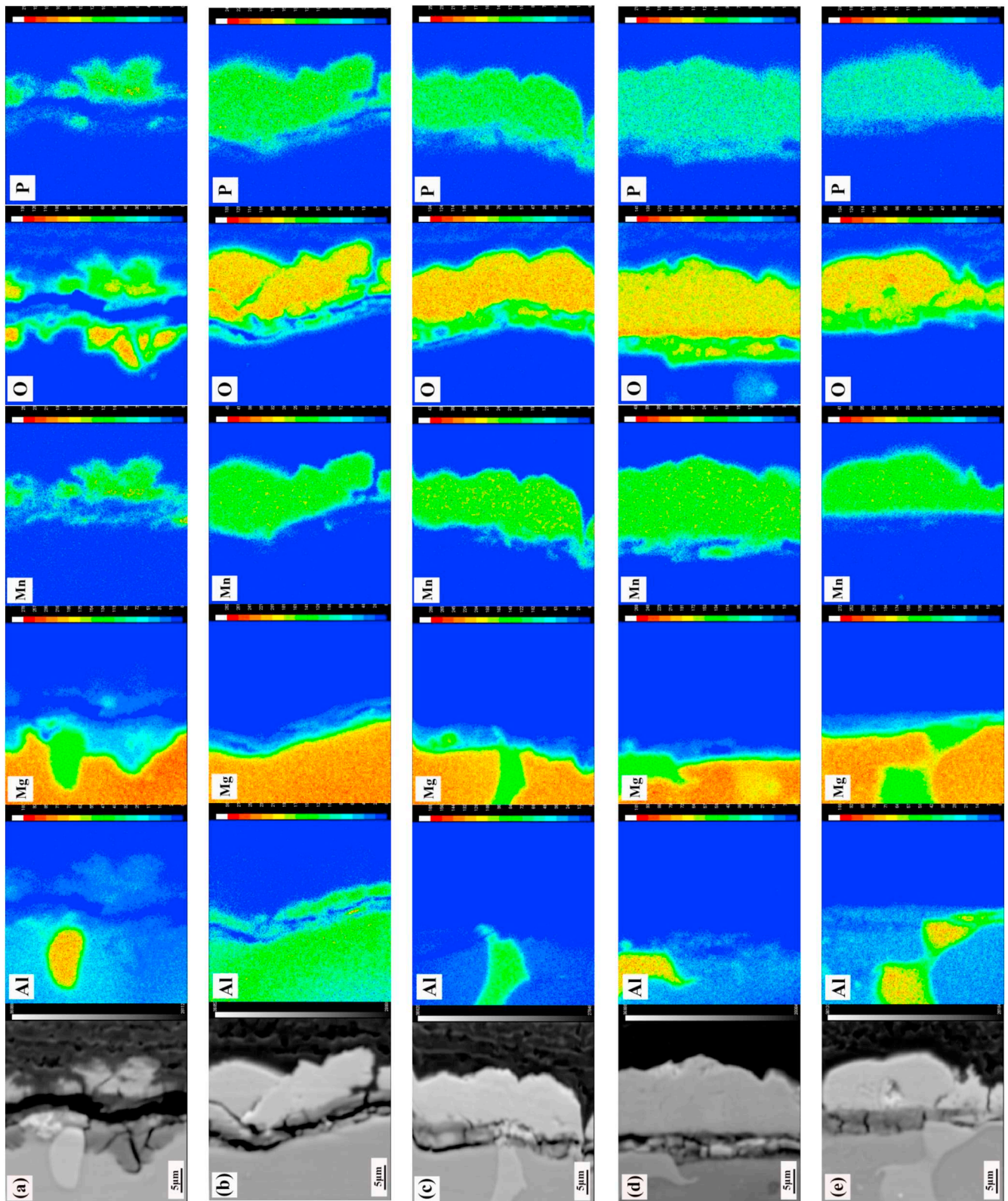


Fig. 7. EMPA mapping of the cross section of the conversion coatings: (a) PCC (sand-blasting), (b) PCC (150 grit), (c) PCC (400 grit), (d) PCC (1000 grit) and (e) PCC (polishing).

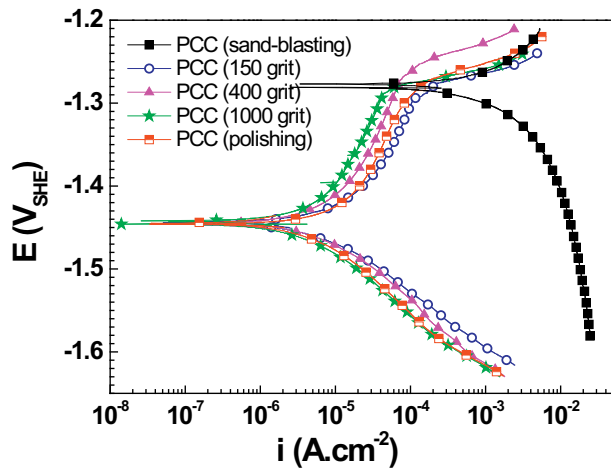


Fig. 8. Polarization curves of the conversion coatings in 3.5 wt% NaCl solution.

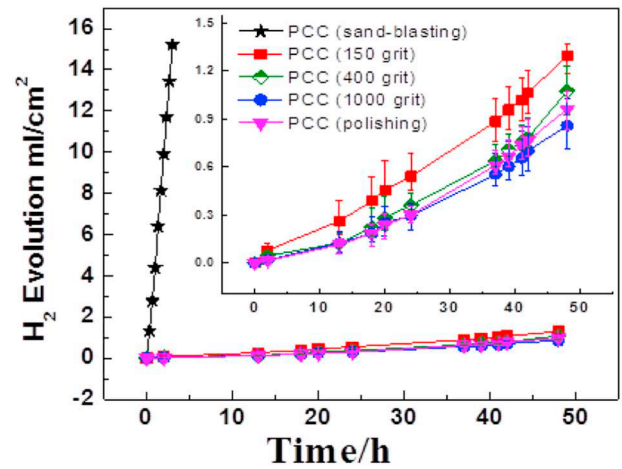


Fig. 9. Hydrogen evolution testing of the conversion coatings in 3.5 wt% NaCl solution.

Table 1

Corrosion current density and corrosion potential of the conversion coatings in 3.5% NaCl solution.

| Specimen | i_{corr} ($\mu\text{A}\cdot\text{cm}^{-2}$) | E_{corr} (mV) |
|---------------------|--|------------------------|
| PCC (sand-blasting) | 3920 ± 46.12 | -1446 ± 12 |
| PCC (150 grit) | 6.91 ± 1.14 | -1438 ± 8 |
| PCC (400 grit) | 6.21 ± 0.91 | -1442 ± 9 |
| PCC (1000 grit) | 3.85 ± 0.78 | -1446 ± 11 |
| PCC (polishing) | 4.86 ± 0.52 | -1445 ± 17 |

roughness, the coating grows uniformly on the Mg alloy surface at the beginning and thus results in a homogenous and protective coating (Fig. 12). It is also noteworthy that the roughness and uniformity of the conversion coating have a huge influence on the adhesion and corrosion performance of the top coating when PCC is used as primer in a protective coating system. The corrosion resistance of conversion coating is related to the corrosion performance and surface roughness of the Mg substrate, implying that a rough substrate results in porous PCC with inferior corrosion protection performance. Moreover, the microstructure and corrosion property of PCC is also determined by the electrochemical surface activity of the substrate, which can be confirmed by PCC (sand-blasting) and PCC (polishing). The Mg dissolution rate and H_2 evolution rate of the sand-blasted sample is relatively fast during coating formation process due to the micro-galvanic corrosion between the newly-formed recrystallized β phase and α -Mg, leading to formation of the non-uniform and porous layer. In the case of ground/polished Mg alloy samples, relatively low surface roughness of the substrate facilitates formation of uniform and corrosion protective phosphate conversion coatings. Therefore, the growth process, microstructure and corrosion protection performance of the conversion

coating is dominated by the surface roughness and electrochemical activity of the Mg alloy base substrate, which can be controlled and altered by surface pretreatment process.

5. Conclusions

It was proved that the surface roughness and electrochemical activity can be altered by surface pre-conditioning treatment, which in turn influence the microstructure and corrosion protection of the phosphate conversion coatings on AZ91 Mg alloy. The morphology and electrochemical activity of the Mg alloy surface has been greatly modified by sand-blasting pretreatment process, which induces severe micro-galvanic corrosion between the newly formed β phase and α -Mg and thus accelerates the corrosion rate of the uncoated and coated Mg alloy. As for the ground/polished alloy, the conversion coating becomes more uniform and denser with the decrease of the surface roughness. The findings are of great importance to select a proper surface pretreatment process before application of conversion coatings and are highly relevant for industrial surface treatments of Mg alloys.

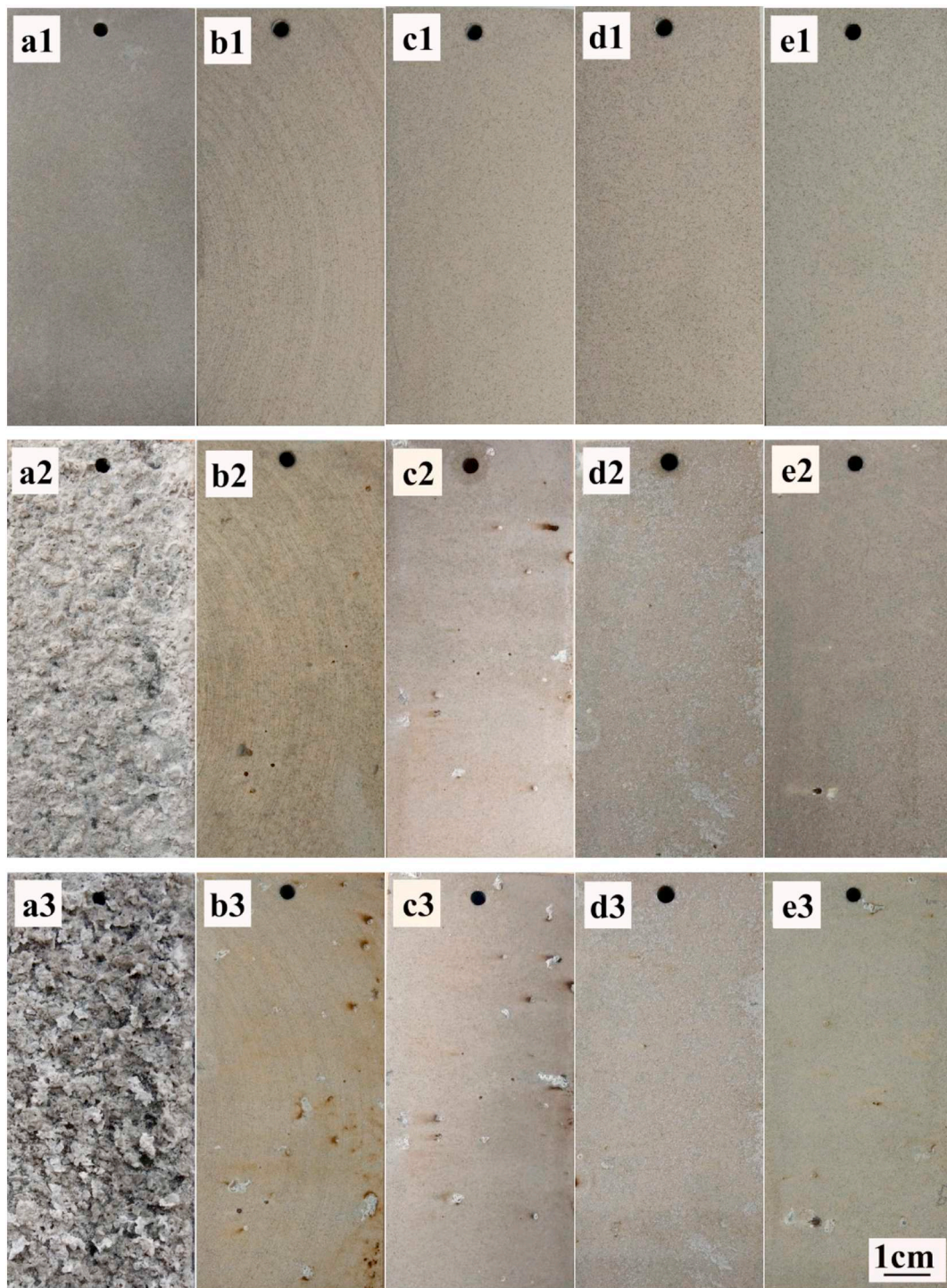


Fig. 10. Macroscopic morphology of the conversion coatings before (a1–e1) and after salt spray test for 48 h (a2–e2) and 72 h (a3–e3). (a) PCC (sand-blasting), (b) PCC (150 grit), (c) PCC (400 grit), (d) PCC (1000 grit) and (e) PCC (polishing).

Table 2
Electrochemical and chemical reactions during formation of PCC.

| | | |
|---------------------------|--|--|
| Electrochemical reactions | Anodic reaction | $Mg \rightarrow Mg^{2+} + 2e$ |
| | Cathodic reaction | $2H^+ + 2e \rightarrow H_2\uparrow$ |
| Intermediate reactions | $H_2PO_4^-$ ionization | $H_2PO_4^- \rightarrow HPO_4^{2-} + H^+$ |
| | HPO_4^{2-} ionization | $HPO_4^{2-} \rightarrow PO_4^{3-} + H^+$ |
| Chemical reactions | Reaction of Mg^{2+} and OH^- | $Mg^{2+} + 2OH^- \rightarrow MgO + H_2O$ |
| | Reaction of Mg^{2+} and HPO_4^{2-} | $Mg^{2+} + HPO_4^{2-} \rightarrow MgHPO_4$ |
| | Reaction of Mn^{2+} and HPO_4^{2-} | $Mn^{2+} + HPO_4^{2-} \rightarrow MnHPO_4$ |

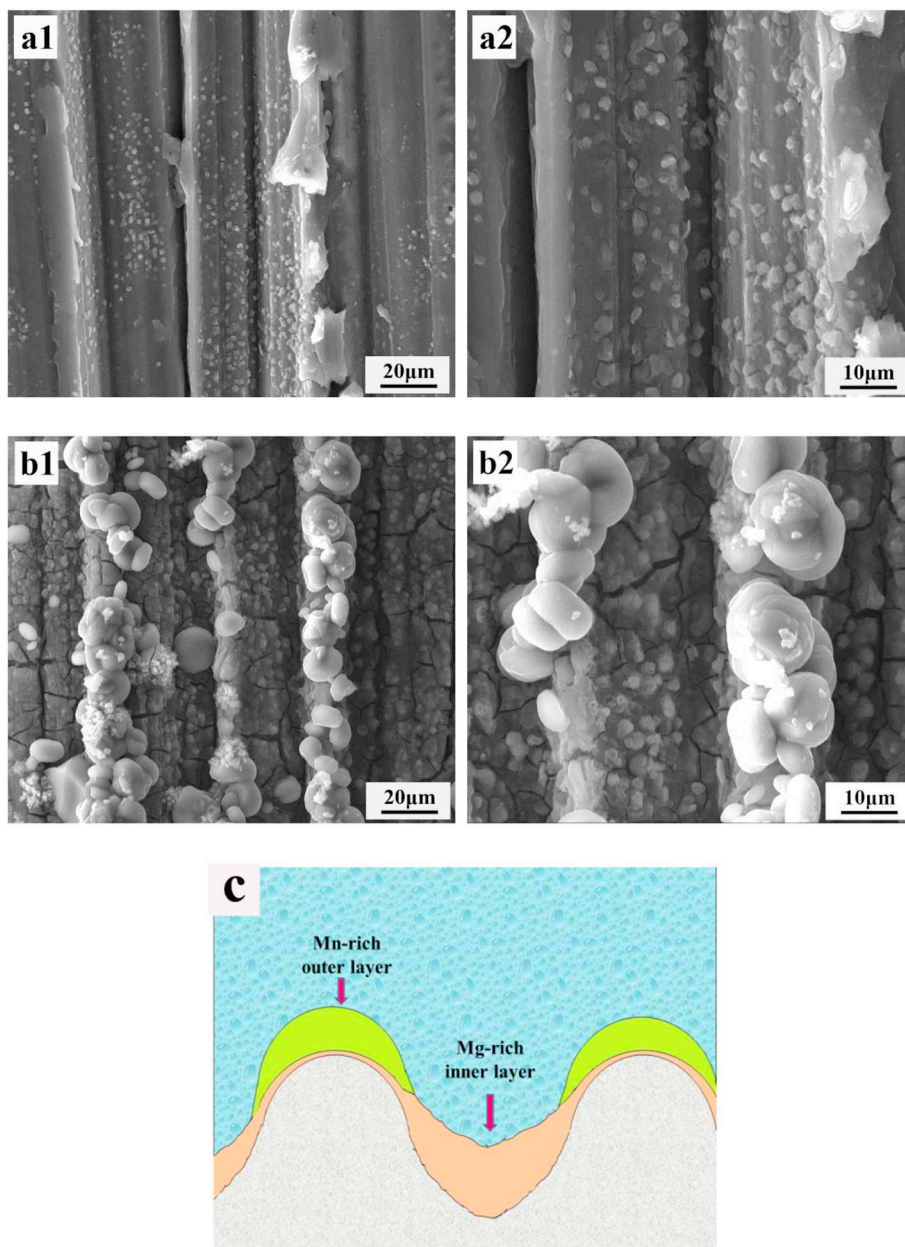


Fig. 11. Surface morphology of PCC (150 grit) during coating formation process. (a) 10 s, (b) 180 s and (c) schematic diagram of the coating formed on Mg alloy with high surface roughness.

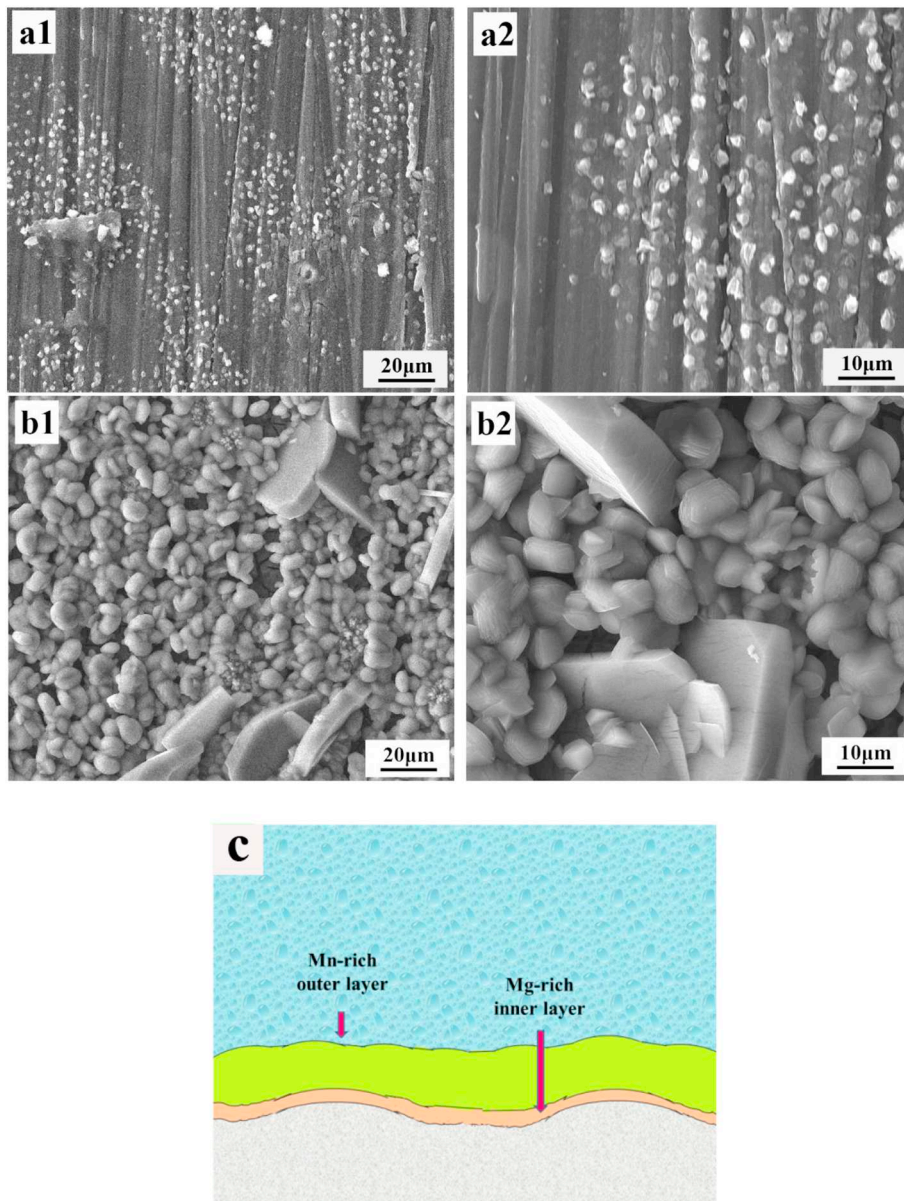


Fig. 12. Surface morphology of PCC (1000 grit) during coating formation process. (a) 10 s, (b) 180 s and (c) schematic diagram of the coating formed on Mg alloy with low surface roughness.

Acknowledgements

The authors would like to acknowledge the financial support of the National Natural Science Foundation of China (NO. 51531007, 51771050 and U1737102), Young Elite Scientists Sponsorship Program by CAST (2017QNRC001), National Program for Young Top-notch Professionals, Fundamental Research Funds for the Central Universities (N170205002 and N170203006) and the International Exchange Program of Harbin Engineering University for Innovation-oriented Talents Cultivation.

References

- [1] C. Ke, Y. Wu, Y. Qiu, J. Duan, N. Birbilis, X.-B. Chen, Influence of surface chemistry on the formation of crystalline hydroxide coatings on Mg alloys in liquid water and steam systems, *Corros. Sci.* 113 (2016) 145–159.
- [2] X. Lu, C. Blawert, Y. Huang, H. Ovri, M.L. Zheludkevich, K.U. Kainer, Plasma electrolytic oxidation coatings on Mg alloy with addition of SiO₂ particles, *Electrochim. Acta* 187 (2016) 20–33.
- [3] M. Esmaily, J.E. Svensson, S. Fajardo, N. Birbilis, G.S. Frankel, S. Virtanen, R. Arrabal, S. Thomas, L.G. Johansson, Fundamentals and advances in magnesium alloy corrosion, *Prog. Mater. Sci.* 89 (2017) 92–193.
- [4] X. Lu, C. Blawert, D. Tolnai, T. Subroto, K.U. Kainer, T. Zhang, F. Wang, M.L. Zheludkevich, 3D reconstruction of plasma electrolytic oxidation coatings on Mg alloy via synchrotron radiation tomography, *Corros. Sci.* 139 (2018) 395–402.
- [5] B.J. Wang, D.K. Xu, J.H. Dong, W. Ke, Effect of corrosion product films on the in vitro degradation behavior of Mg-3%Al-1%Zn (in wt%) alloy in Hank's solution, *J. Mater. Sci. Technol.* 34 (2018) 1756–1764.
- [6] Y.C. Su, Y.C. Su, Y.B. Lu, J.S. Lian, G.Y. Li, Composite microstructure and formation mechanism of calcium phosphate conversion coating on magnesium alloy, *J. Electrochem. Soc.* 163 (2016) G138–G143.
- [7] X. Lu, M. Mohedano, C. Blawert, E. Matykina, R. Arrabal, K.U. Kainer, M.L. Zheludkevich, Plasma electrolytic oxidation coatings with particle additions – a review, *Surf. Coat. Technol.* 307 (Part C) (2016) 1165–1182.
- [8] L.-Y. Cui, H.-P. Liu, W.-L. Zhang, Z.-Z. Han, M.-X. Deng, R.-C. Zeng, S.-Q. Li, Z.-L. Wang, Corrosion resistance of a superhydrophobic micro-arc oxidation coating on Mg-4Li-1Ca alloy, *J. Mater. Sci. Technol.* 33 (2017) 1263–1271.
- [9] Y. Chen, X. Lu, C. Blawert, M.L. Zheludkevich, T. Zhang, F. Wang, Formation of self-lubricating PEO coating via in-situ incorporation of PTFE particles, *Surf. Coat. Technol.* 337 (2018) 379–388.
- [10] D. Mei, S.V. Lamaka, J. Gonzalez, F. Feyerabend, R. Willumeit-Römer, M.L. Zheludkevich, The role of individual components of simulated body fluid on the corrosion behavior of commercially pure Mg, *Corros. Sci.* (2018), <https://doi.org/10.1016/j.corsci.2018.11.011>.

- [11] C.S. Lin, S.K. Fang, Formation of cerium conversion coatings on AZ31 magnesium alloys, *J. Electrochem. Soc.* 152 (2005) B54–B59.
- [12] X.B. Chen, N. Birbilis, T.B. Abbott, Review of corrosion-resistant conversion coatings for magnesium and its alloys, *Corrosion* 67 (3) (2011).
- [13] J. Chen, Y. Song, D. Shan, E.-H. Han, Study of the in situ growth mechanism of Mg–Al hydrotalcite conversion film on AZ31 magnesium alloy, *Corros. Sci.* 63 (2012) 148–158.
- [14] J. Cerezo, I. Vandendael, R. Posner, K. Lill, J.H.W. de Wit, J.M.C. Mol, H. Terryn, Initiation and growth of modified Zr-based conversion coatings on multi-metal surfaces, *Surf. Coat. Technol.* 236 (2013) 284–289.
- [15] E. Saei, B. Ramezanzadeh, R. Amini, M.S. Kalajahi, Effects of combined organic and inorganic corrosion inhibitors on the nanostructure cerium based conversion coating performance on AZ31 magnesium alloy: morphological and corrosion studies, *Corros. Sci.* 127 (2017) 186–200.
- [16] N.V. Phuong, K.H. Lee, D. Chang, S. Moon, Effects of Zn^{2+} concentration and pH on the zinc phosphate conversion coatings on AZ31 magnesium alloy, *Corros. Sci.* 74 (2013) 314–322.
- [17] X.B. Chen, D.R. Nisbet, R.W. Li, P.N. Smith, T.B. Abbott, M.A. Easton, D.H. Zhang, N. Birbilis, Controlling initial biodegradation of magnesium by a biocompatible strontium phosphate conversion coating, *Acta Biomater.* 10 (2014) 1463–1474.
- [18] H.H. Elsentriecy, K. Azumi, H. Konno, Improvement in stannate chemical conversion coatings on AZ91 D magnesium alloy using the potentiostatic technique, *Electrochim. Acta* 53 (2007) 1006–1012.
- [19] Q. Li, S. Xu, J. Hu, S. Zhang, X. Zhong, X. Yang, The effects to the structure and electrochemical behavior of zinc phosphate conversion coatings with ethanolamine on magnesium alloy AZ91D, *Electrochim. Acta* 55 (2010) 887–894.
- [20] T. Yan, L. Tan, B. Zhang, K. Yang, Fluoride conversion coating on biodegradable AZ31B magnesium alloy, *J. Mater. Sci. Technol.* 30 (2014) 666–674.
- [21] C.S. Lin, C.Y. Lee, W.C. Li, Y.S. Chen, G.N. Fang, Formation of phosphate/per-manganate conversion coating on AZ31 magnesium alloy, *J. Electrochem. Soc.* 153 (2006) B90–B96.
- [22] Y. Song, D. Shan, R. Chen, F. Zhang, E.-H. Han, Formation mechanism of phosphate conversion film on Mg–8.8Li alloy, *Corros. Sci.* 51 (2009) 62–69.
- [23] Y.C. Yang, C.Y. Tsai, Y.H. Huang, C.S. Lin, Formation mechanism and properties of titanate conversion coating on AZ31 magnesium alloy, *J. Electrochem. Soc.* 159 (2012) C226–C232.
- [24] M.P. Brady, D.N. Leonard, H.M. Meyer Iii, J.K. Thomson, K.A. Unocic, H.H. Elsentriecy, G.L. Song, K. Kitchen, B. Davis, Advanced characterization study of commercial conversion and electrocoating structures on magnesium alloys AZ31B and ZE10A, *Surf. Coat. Technol.* 294 (2016) 164–176.
- [25] Y.H. Huang, Y.L. Lee, C.S. Lin, Acid pickling pretreatment and stannate conversion coating treatment of AZ91D magnesium alloy, *J. Electrochem. Soc.* 158 (2011) C310–C317.
- [26] Y.L. Lee, F.J. Chen, C.S. Lin, Corrosion resistance studies of cerium conversion coating with a fluoride-free pretreatment on AZ91D magnesium alloy, *J. Electrochem. Soc.* 160 (2013) C28–C35.
- [27] M. Zhao, J.G. Li, G.P. He, H.L. Xie, Y.A. Fu, Nano Al_2O_3 /phosphate composite conversion coating formed on magnesium alloy for enhancing corrosion resistance, *J. Electrochem. Soc.* 160 (2013) C553–C559.
- [28] J. Cerezo, P. Taheri, I. Vandendael, R. Posner, K. Lill, J.H.W. de Wit, J.M.C. Mol, H. Terryn, Influence of surface hydroxyls on the formation of Zr-based conversion coatings on AA6014 aluminum alloy, *Surf. Coat. Technol.* 254 (2014) 277–283.
- [29] J. Cerezo, I. Vandendael, R. Posner, J.H.W. de Wit, J.M.C. Mol, H. Terryn, The effect of surface pre-conditioning treatments on the local composition of Zr-based conversion coatings formed on aluminium alloys, *Appl. Surf. Sci.* 366 (2016) 339–347.
- [30] G. Duan, L. Yang, S. Liao, C. Zhang, X. Lu, Y. Yang, B. Zhang, Y. Wei, T. Zhang, B. Yu, X. Zhang, F. Wang, Designing for the chemical conversion coating with high corrosion resistance and low electrical contact resistance on AZ91D magnesium alloy, *Corros. Sci.* 135 (2018) 197–206.
- [31] K. Lu, J. Lu, Surface nanocrystallization (SNC) of metallic materials-presentation of the concept behind a new approach, *J. Mater. Sci. Technol.* 15 (1999) 193–197.
- [32] R. Zeng, Z. Lan, L. Kong, Y. Huang, H. Cui, Characterization of calcium-modified zinc phosphate conversion coatings and their influences on corrosion resistance of AZ31 alloy, *Surf. Coat. Technol.* 205 (2011) 3347–3355.
- [33] X.-B. Chen, X. Zhou, T.B. Abbott, M.A. Easton, N. Birbilis, Double-layered manganese phosphate conversion coating on magnesium alloy AZ91D: insights into coating formation, growth and corrosion resistance, *Surf. Coat. Technol.* 217 (2013) 147–155.
- [34] X. Lu, Y. Chen, C. Zhang, T. Zhang, B. Yu, H. Xu, F. Wang, Formation mechanism and corrosion performance of phosphate conversion coatings on AZ91 and Mg-Gd-Y-Zr alloy, *J. Electrochem. Soc.* 165 (2018) C601–C607.
- [35] M.H. Moayed, N.J. Laycock, R.C. Newman, Dependence of the critical pitting temperature on surface roughness, *Corros. Sci.* 45 (2003) 1203–1216.